Synthesis, characterization, fluorescence and computational studies of new Cu2+, Ni2+ and Hg2+ complexes with emissive thienylbenzoxazolyl–alanine ligands

ARTICLE *in* INORGANICA CHIMICA ACTA · JANUARY 2011

Impact Factor: 2.05 · DOI: 10.1016/j.ica.2010.10.025

Inorganica Chimica Acta 366 (2011) 154–160

Contents lists available at ScienceDirect

Inorganica Chimica Acta

journal homepage: www.elsevier.com/locate/ica

Synthesis, characterization, fluorescence and computational studies of new Cu^{2+}, Ni^{2+} and Hg^{2+} complexes with emissive thienylbenzoxazolyl-alanine ligands

Elisabete Oliveira [a], S.P.G. Costa [b,*], M.M.M. Raposo [b], Olalla Nieto Faza [c], Carlos Lodeiro [a,d,*]

[a] REQUIMTE, Department of Chemistry, FCT-UNL, 2829-516 Monte de Caparica, Portugal
[b] CQ-UM, Center of Chemistry, University of Minho, Campus de Gualtar, 4710-057 Braga, Portugal
[c] Faculty of Science, Organic-Chemistry Department, Campus Ourense, University of Vigo, 32004 Ourense, Spain
[d] BIOSCOPE Research Team, Faculty of Science, Physical-Chemistry Department, Campus Ourense, University of Vigo, 32004 Ourense, Spain

ARTICLE INFO

Article history:
Received 9 July 2010
Received in revised form 17 October 2010
Accepted 24 October 2010
Available online 2 November 2010

Keywords:
Mercury(II)
Copper(II)
Benzoxazole
Thiophene
Alanine derivatives
Emissive compounds

ABSTRACT

The interaction of four fluorescent compounds containing thiophene and benzoxazole moieties combined with an alanine residue with alkaline, alkaline-earth, transition and post-transition metal ions was explored. The highly fluorescent heterocyclic alanine derivatives are strongly quenched in the solid state after complexation with the paramagnetic metal ions Cu^{2+} and Ni^{2+}, and with the diamagnetic Hg^{2+}. Absorption and steady-state fluorescence titrations reveal a selective interaction with Cu^{2+}, Ni^{2+} and Hg^{2+}. In all cases the formation of mononuclear or dinuclear metal complexes in solid state and in solution are postulated. DFT calculations on the mercury(II) complexes confirm the formation of dinuclear species. Our results suggest that one metal ion is coordinated by the chelate group formed by the amine and the protonated carboxylic groups present in the amino acid residue while a second metal ion is directly linked to the chromophore. As parent compound, L4 shows no interaction with Cu^{2+} and Ni^{2+} salts. However, the interaction with Hg^{2+} induces a strong quenching and a red shift of the fluorescence emission.

1. Introduction

The interactions of amino acids or peptides with transition metals have been extensively investigated due to their importance as multifunctional materials in biology, pharmacy and industry [1]. Many of these metal complexes show versatile properties including antibacterial, antitumor, or anticancer activities [2–5]. As is well known, many types of enzymes contain metal ions as cofactors, and in order to understand some of these biological processes, the interaction of metal complexes containing amino acids have been studied [6]. In this set of applications, Grosser et al. have recently concluded that the alanine residue has an anti-oxidant action [7].

In the field of peptide mass mapping (Proteomics approach), transition metal complexes can be used as cleavage reagents for peptides and proteins [8–12]. With this aim, several Pd^{2+} complexes with small peptides containing histidine and methionine as amino acids have been recently shown to promote a hydrolytic cleavage of these residues [13]. Copper(II) is one of the most interesting transition metal ions in biologic fields due to the participation in electron transfer processes in proteins containing hydrophobic sites [14]. In this way, Marine et al. have published some interesting theoretical studies on the interaction of Cu^{2+} with alanine amino acids, their results showing that Cu^{2+} ions are preferentially linked to the C-terminal carboxylate group of the alanine residue [15].

In the present work we have combined the design of new fluorescent materials based on bio-inspired ligands with transition and pollutant heavy metal ions such as Cu^{2+}, Ni^{2+} and Hg^{2+} as potential proteomics platforms in the broader context of our research lines on fluorescence and colorimetric chemosensors [16–19].

These compounds show selectivity, towards Cu^{2+}, Ni^{2+} and Hg^{2+} over other metals including Zn^{2+}, Ca^{2+}, Na^{+} in solution [17]. Here we report the synthesis of eight new Cu^{2+}, Ni^{2+} and Hg^{2+} metal complexes with ligands L1, L2 and L3 (Scheme 1), their characterization, and spectroscopic and DFT studies. For comparative purposes, we also present the photophysical studies with metal ions using the *bis*-alanine L4, which contains two moieties of benzoxazolylalanine linked through a thiophene spacer (Scheme 1).

2. Results and discussion

2.1. Synthesis and characterization. Complexation studies

The synthesis of L1, L2 and L3 was previously reported by us [17,18], while L4 was obtained by a standard deprotection procedure from the methyl ester parent compound [19].

* Corresponding authors. Address: BIOSCOPE Research Team, Faculty of Science, Physical-Chemistry Department, Campus Ourense, University of Vigo, 32004 Ourense, Spain (C. Lodeiro). Tel.: +34 988 387072; fax: +34 988 387001.
E-mail addresses: spc@quimica.uminho.pt (S.P.G. Costa), faza@uvigo.es (O.N. Faza), clodeiro@uvigo.es (C. Lodeiro).

0020-1693/$ - see front matter © 2010 Elsevier B.V. All rights reserved.
doi:10.1016/j.ica.2010.10.025

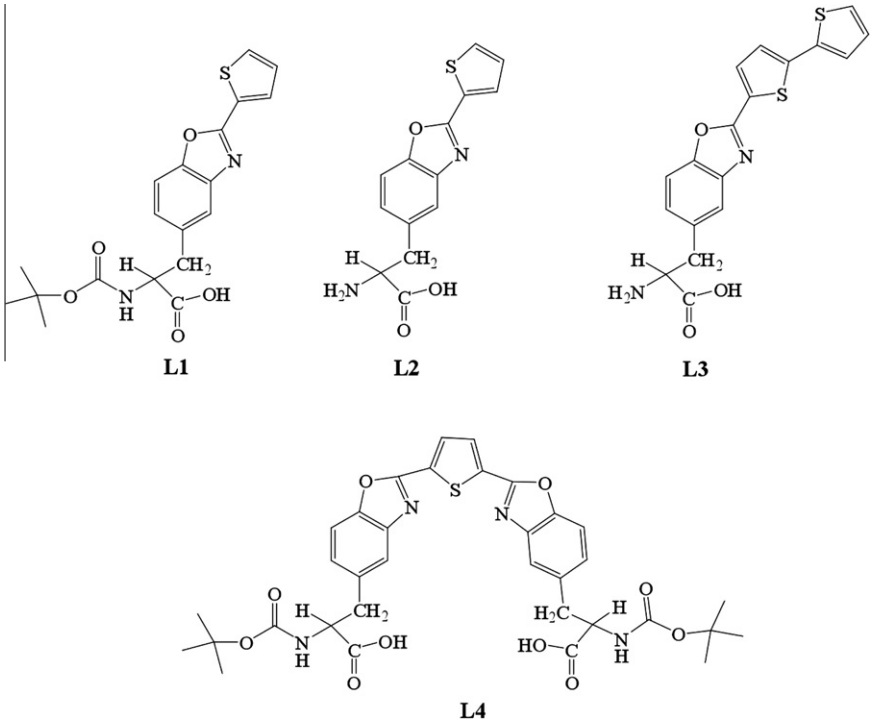

Scheme 1. Structure of benzoxazolyl-alanine derivatives studied.

The synthesis of the metal complexes of L1, L2 and L3 with the hydrated metal salts [M = Cu^{2+}, Ni^{2+} and Hg^{2+} X = CF_3SO_3 or BF_4] was studied in absolute ethanol by direct reactions, leading to the formation of complexes with 1:1 or 2:1 metal-to-ligand ratio. The pure analytical complexes gave formula: $[Cu_2L1](CF_3SO_3)_4{\cdot}2CH_3CN{\cdot}2H_2O$ **(1)**, $[Ni_2L1](BF_4)_4{\cdot}7H_2O$ **(2)**, $[Hg_2L1](CF_3SO_3)_4{\cdot}4H_20$ **(3)**, $[Cu_2L2](CF_3SO_3)_4{\cdot}3H_2O$ **(4)**, $[Ni_2L2](BF_4)_4{\cdot}6H_2O$ **(5)**, $[Hg_2L2](CF_3SO_3)_4{\cdot}2CH_3CN{\cdot}2H_2O$ **(6)**, $[Ni_2L3](BF_4)_4{\cdot}4H_2O$ **(7)** and $[Cu_2L3]$ $(CF_3SO_3)_4{\cdot}3H_2O$ **(8)**.

All colored solid complexes are air-stable and soluble in absolute ethanol, acetonitrile, DMSO, dichloromethane and chloroform.

All complexes were characterized by elemental analysis, IR, ^1H NMR, UV–Vis, fluorescence and matrix-assisted laser desorption ionization time-of-flight (MALDI-TOF-MS) spectroscopy. To confirm the number of metal ions in each complex the amount of metal was determined by atomic absorption spectrometry following several methods previously reported [20].

The IR spectra registered in KBr pellets show similar bands attributed to the ν(C=N) and ν(C=C) stretching modes of the aromatic rings appear at 1619–1925 and at 1574–1579, respectively. As far as the counter ions are concerned, in all the BF_4 complexes four bands were observed at 777, 360, 1070 and 533 cm^{-1} and assigned to the four actives ν1, ν2, ν3, and ν4 vibrational modes, respectively [22]. In the triflate complexes the intense band at 1280 cm^{-1}, associated with the vibrational tension band ν_{as}(S–O) corroborated the ionic presence of these anions [21]. These results suggest that both kinds of counterions are not involved in coordination to the metal ions. The appearance of a broad band at around 3400 cm^{-1} in all complexes indicates the presence of coordinated and/or hydrated water molecules [21]. This result is in agreement with the DFT studies where the metal ions are stabilized by completing the coordination sphere with water.

MALDI-TOF-MS spectra of the complexes (see experimental section) display peaks corresponding to $[M\mathbf{L}]^+$, $[M\mathbf{L}X]^+$, $[M\mathbf{L}X_2]^+$, $[M_2\mathbf{L}X]^+$ and $[M_2\mathbf{L}X_3]^+$ fragments, which indicates the integrity of the alanine derivatives and the presence of the metal ions in the complexes.

As was pointed above the ^1H NMR spectra of the mercury(II) complexes were registered in DMSO-d_6 at room temperature. The signals observed were broad in comparison with those in the free ligand due to the complexation effect. However, all-important peaks attributed to the amino-acid moiety were observed confirming the integrity of the ligand in the metal complex. The most affected peaks were assigned to the aromatic chromophores.

All free ligands are very emissive in the solid state (see Fig. 1). The strong emission band is centered at *ca.* 400, 430 and 485 nm for L1, L2 and L3, respectively. In the particular case of L1, the emission band showed a long tail centred at 500 nm that could be assigned to some intermolecular interactions between ligands in the ground state.

The fluorescence spectra of the solid complexes **1–8** were obtained exciting the samples at 315 nm. With respect to those of the ligands these spectra are in general highly quenched, with the exception of the Cu^{2+} and Ni^{2+} complexes with L2 and L3 (see Fig. 1 panels B and C).

This quenching confirms the formation of the metal complexes. It is due to the energy transfer from the π^* emissive state of the ligand though low-lying metal-centre, and the heavy metal effect in the case of Hg^{2+} inducing an effective intersystem crossing mechanism [23–25] suggests that the metal interacts with the chromophore units. This observation was later confirmed by DFT studies.

2.2. Computational methods

DFT was used to optimize the geometries of L2 and the L2:Hg^{2+} and L2:Hg_2^{2+} complexes (See Fig. 2). Since different coordination spheres can surround mercury, one to three explicit water molecules were included as co-ligands in the preliminar work. The following energetic discussion, however, only refers to the species with one water molecule, since only the tri-coordinate species were found to be stable with water (other water molecules leave the coordination site along the optimization). In order to stabilize a four-coordinated mercury complex it was necessary to use other co-ligands such as an acetonitrile molecule (see Fig. 2).

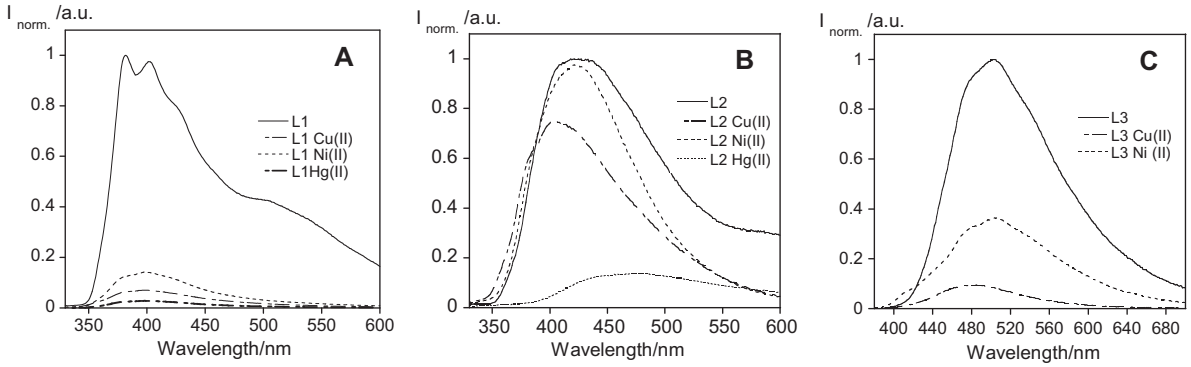

Fig. 1. Solid-state emission spectra of L1(A), L2(B) and L3(C) and its corresponding metal complexes with Cu^{2+}, Ni^{2+} and Hg^{2+} ($\lambda_{excL1,L2}$ = 315 nm, λ_{excL3} = 366 nm, T = 298 K).

The 1:1 (ML) complex is stabilized by 33 kcal/mol with respect to the free ligand and the $Hg(H_2O)_2^{2+}$ cation. The first metal cation is coordinated to both the deprotonated carboxylate and the amine of the alanine group, as expected. The coordination of this first cation to the sulfur and nitrogen on the aromatic part of L2 would only be favored by 7.5 kcal/mol when compared to the free species, and even by less when the coordination site is formed by S and O (see Table 1).

Coordination of two metal units is favoured by 33 kcal/mol with respect to the free fragments, and by about 1 kcal/mol with respect to the L2:$Hg(H_2O)$ complex, water and a further $Hg(H_2O)_2$ complex. In this case, there is a strong preference for S,N coordination, rather than the alternative complexation to S,O, that results in a energy difference between the L2:$[Hg(H_2O)]_2$_SN and L2:$[Hg(H_2O)]_2$_SO complexes of about 17 kcal/mol. The coordination to the heteroatoms in the aromatic part of the ligand is not always symmetric. In the structures where L2 is chelating mercury through sulphur and nitrogen, the interaction is much stronger with the nitrogen atom, both in terms of bond distances (Hg–N distance of 2.20 Å and Hg–S distance of 3.65 Å) and the NBO bond orders (0.31 and 0.02, respectively). In the case of S,O coordination, there are two structures within a 1 kcal/mol energy region. In one of them (L2:$[Hg(H_2O)]_2$_SO), the metal is bonded to the sulphur atom (3.07 Å, bond order of 0.14) with only electrostatic contributions to the O-Hg bonding (3.40 Å and 0.02 bond order). In the other structure (L2:$[Hg(H_2O)]_2$_SO_2), the metal center displays a stronger interaction with the oxygen (Hg–S distance of 3.65 Å and Hg–O distance of 2.99 Å, with bond orders, respectively).

Although not common, other examples of tricoordinate mercury can be found in the literature [26], usually with sulphur and two halogens as ligands. In exploratory gas phase calculations, protonation of the aminoacid carboxilate is needed to achieve a stable L2:$Hg(H_2O)_2$ complex with a distorted trigonal pyramid geometry. As was pointed above, this increase in the allowed coordination

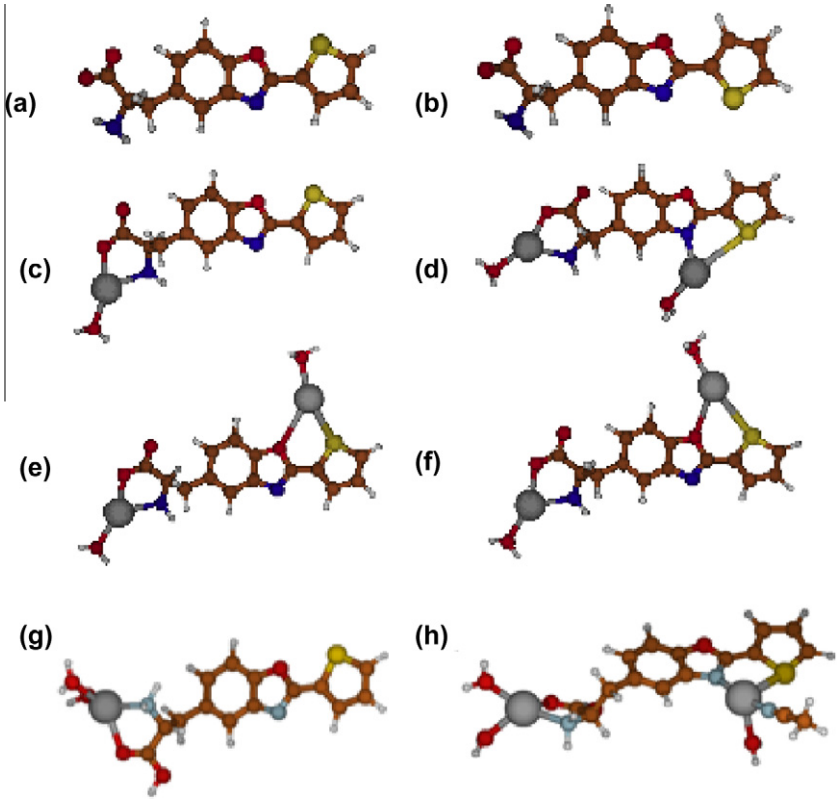

Fig. 2. DFT structures of ligand L2 in the presence of one and two equivalents of Hg(II).

Table 1
DFT (CAM-B3LYP/def2-svp (PCM, ethanol)) electronic and free energies in kcal/mol for the mercury-L2 complexes studied. The relative values have been calculated with respect to $Hg(H_2O)_2^{2+}$, the free ligand L2, and H_2O.

Structure	Electronic energy	ΔG	Relative electronic energy	Relative DG
H_2O	−47901.77	−47899.46		
$Hg(H_2O)_2$	−191907.38	−191894.45		
L2_1	−798476.02	−798359.04		
L2_2	−798476.50	−798359.31		
L2:$Hg(H_2O)$	−942514.77	−942383.09	−32.66	−28.80
L2:$Hg(H_2O)$_SN	−942492.62	−942361.83	−10.50	−7.54
L2:$Hg(H_2O)$_SO	−942473.18	−942344.47	8.93	9.82
L2:$[Hg(H_2O)]_2$_SN	−1086522.80	−1086377.38	−35.07	−36.09
L2:$[Hg(H_2O)]_2$_SO	−1086505.26	−1086360.35	−17.53	−19.30
L2:$[Hg(H_2O)]_2$_SO_2	−1086505.13	−1086358.87	−17.40	−18.63

number of mercury as a result of the lesser basicity of the ligands, is also found when a water molecule is replaced by acetonitrile on the second mercury cation, coordinated to the heterocyclic region of L2 (see Fig. 2). Thus, a structure could be optimized where Hg^{2+} coordinates to the sulphur and nitrogen atoms on L2, completing its coordination sphere with one water and one acetonitrile molecule, also arrayed in a distorted trigonal pyramid, while this same fourth coordination site would not accept a water molecule. In this case, with a non-deprotonated alanine coordinating a Hg^{2+} center with two attached water molecules, a second Hg^{2+} cation with one water and one acetonitrile as ligands also prefers to coordinate to the chromophore through its N,S atoms instead of doing it through O,S. This preferece for nitrogen over oxygen coordination in this system has a value of about 8 kcal/mol and, in fact, Hg^{2+} with two ligands doesn't bind to the heterocyclic oxygen, resulting in a new tricoordinate T-shaped moiety in contrast to the pyramidal S,N complex.

Thus, independently of the exact model chosen for the ligand (protonated or deprotonated aminoacid residue) or for the exact coordination sphere of the metal, these theoretical studies support the coordination proposed by resorting to UV–Vis and Fluorescence spectroscopy: (i) the first metal center coordinates to the alanine moiety, and (ii) interaction with the aromatic chromophore is observed at larger metal concentrations.

2.3. Spectroscopyc studies

In our previous study we have reported using ligands L1 and L2 as fluorescent probes in solution, for the detection of Na^+, Ca^{2+}, Zn^{2+}, Hg^{2+}, Cu^{2+} and Ni^{2+} [17]. In these cases only a selective interaction with Hg^{2+}, Cu^{2+} and Ni^{2+} was observed. Based on these results, now, we have evaluated the sensor capability of ligands L3 and L4 towards the same metal ions by UV–Vis and fluorescence metal titrations using absolute ethanol or dichloromethane as solvents.

As can be seen in Scheme 1, compounds L1 and L4 have a protecting group at the N-terminal position of the amino residue, thus preventing the metal complexation by the amino group. These compounds were selected as model systems for L2 and L3 in order to better understand the coordination reactions by the carboxyl group and the chromophore.

During the titration of L3 with an ethanolic Hg^{2+} solution, the intensity of fluorescence was dramatically reduced. However, after the first metal additions a white precipitate appears immediately preventing further studies in solution. It is interesting to note that ligand L3 also does not produce good analytical results for the mercury(II) solid complex.

On the other hand as can be seen in Fig. 3, even if the ground state was not affected after metal addition, (spectra do not show), a progressive quenching reaction could be observed in the presence of copper(II) (Fig. 3, panel A) and nickel(II) (Fig. 3, panel B).

The strongest quenching effect was observed for Cu^{2+}; half molar equivalent of metal ion was enough to totally quench the fluorescence emission. This result is unique among all the ligands reported, suggesting the formation in solution of a sandwich complex between two ligands and one metal center. Studies using the Hypspec program [27] confirmed this hypothesis and suggest a complex with log K of 12.81 ± 0.05. Taking into account the strong effect observed in the emission band, we could postulate that the metal center also affects the chromophores of both ligands.

In the titration with nickel(II) the complex obtained shows a ligand–metal stoichiometry of 1:1 with an association constant of 4.62 ± 0.01 (see Table 2), one of the smallest values obtained for these compounds. As can be seen in Fig. 2 the quenching achieved was not complete. In comparison with the previous published complexation constants with ligands L1 and L2 [17], the values obtained for L3 are higher, specially for copper(II).

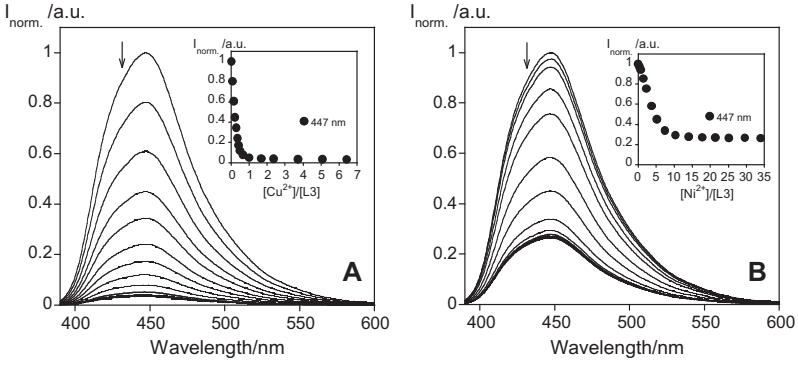

Fig. 3. Spectrofluorimetric titrations (A and B) of ligand L3 in the presence of $Cu(CF_3SO_2)_2$ (A) and $Ni(BF_4)_2$ (B) in absolute ethanol. ([**L3**] = 1.00×10^{-5} M, $[Cu(CF_3SO_2)_2]$ = 1.02×10^{-2} M, $[Ni(BF_4)_2]$ = 1.00×10^{-2} M, T = 298 K, λ_{exc} = 366 nm. (insets: normalized emission at 447 nm).

Ligand L4 results of the combination of a second benzoxazolylalanine moiety with ligand L1. L4 was obtained from a selective C-terminal deprotection of the methyl ester precursor reported previously by us [19]. The sensing ability of L4 towards the same transition metals was explored in order to evaluate the influence of the additional benzoxazolylalanine moiety. The corresponding photophysical characterization is reported in Fig. 4 panel A.

Addition of Cu^{2+} or Ni^{2+} to a dichloromethane solution containing L4, does not modify the absorption and emission spectra. However a strong interaction resulting in a quenching effect was observed for mercury(II), see Fig. 4 panel B and C, affecting both, ground and excited states. In this case, one metal center was enough to totally quench the strong fluorescence emission shown by the free ligand ($\Phi = 0.77$) [19]. The JOB plot experiments confirm the formation of a mononuclear complex (Fig. 4 panel d). After complexation the emission band centered at 440 nm was red shifted to 480 nm and calculations by the Hypspec program gave a value for the complexation constant with a log K of 6.50 ± 0.03.

Table 2
Complexation constants (log K) for benzoxazolyl-alanine ligands L1 to L4 with Cu(II), Ni(II) and Hg(II) in absolute ethanol calculated with Hypspec program.

Compound	Complex[a] Ref.	log K	M:L
L1	L1Cu	3.75 ± 0.05	1:1
	L1Hg[a]	5.01 ± 0.04	1:1
		9.37 ± 0.07	2:1
L2	L2Cu[a]	9.77 ± 0.02	2:1
	L2Hg[a]	7.78 ± 0.02	2:1
L3	L3Cu	12.81 ± 0.05	1:2
	L3Ni	4.62 ± 0.01	1:1
L4	L4Hg	6.50 ± 0.03	1:1

3. Experimental

3.1. Physical measurements

Elemental analyses were performed on a Fisons Instruments EA1108 microanalyser at the Universidade de Vigo. Infra-red spectra were recorded as KBr discs on a JASCO FT-IR 410 spectrophotometer.

MALDI-TOF-MS data were obtained using a MALDI-TOF-MS model Voyager DE-PRO Biospectrometry Workstation equipped with a nitrogen laser irradiating at 337 nm (Applied Biosystems, Foster City, United States) from the MALDI-TOF-MS Service of the REQUIMTE, Chemistry Department, Universidade Nova de Lisboa. The acceleration voltage was 2.0×10^4 kV with a delayed extraction (DE) time of 200 ns. The spectra represent accumulations of 5×100 laser shots. The reflection mode was used. The ion source and flight tube pressures were less than 1.80×10^{-7} and 5.60×10^{-8} Torr, respectively.

The MALDI mass spectra of the soluble samples (1 or 2 mg/mL) such as the ligand and metal complexes were recorded using the conventional sample preparation method for MALDI-MS. In the metal ion titrations by MALDI the metal sample (1 mL) was put on the sample holder on which the chelating ligand **L** had been previously spotted. The sample holder was inserted into the ion source. Chemical reaction between the ligand and metal salts occurred in the holder and complex species were produced.

3.2. Spectrophotometric and spectrofluorimetric measurements

Absorption spectra were recorded on a JASCO 650 spectrophotometer and fluorescence emission on a Horiba-Jovin Ibon Fluoromax 4. The linearity of the fluorescence emission versus concentration was checked in the concentration used (10^{-4}–10^{-6}

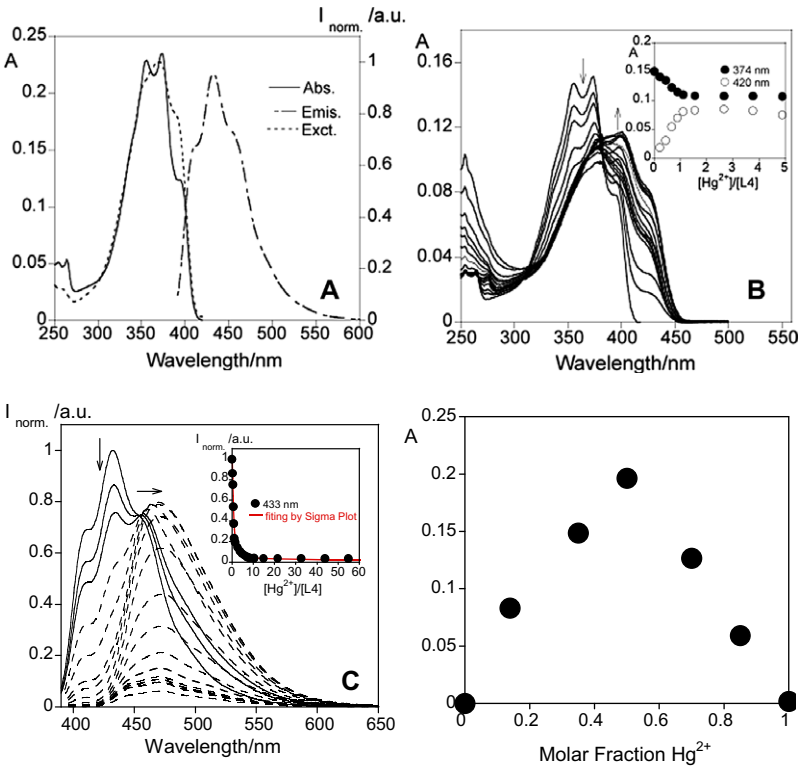

Fig. 4. Absorption, emission and excitation spectra of ligand L4 ($T = 298$ K, [L4] = 1.40×10^{-6} M, $\lambda_{exc} = 374$ nm) (A) and spectrophotometric (B) and spectrofluorimetric titration (C) of L4 with a standard solution of $Hg(CF_3SO_3)_2$ in dichloromethane, ([L4] = 1.40×10^{-6} M, $\lambda_{exc} = 434$ nm, the inset shows the normalized emission at 433 nm, and the fitting by Sigma Plot). Panel D shows the JOB plot for L4/Hg^{2+} interaction.

M). A correction for the absorbed light was performed when necessary. The spectrometric characterizations and titrations were performed as follows: the stock solutions of the compounds (*ca.* 10^{-3} M) were prepared by dissolving an appropriated amount of the ligand in a 10 ml volumetric flask and diluting to the mark with the solvent. The titrated solutions were prepared by appropriate dilution of the stock solutions still 10^{-5}–10^{-6} M. Titrations of the ligand L4 were carried out by the addition of microliter amounts of standard solutions of the ions in dichloromethane (1.40×10^{-6} M).

Fluorescence spectra of solid samples were recorded using a fiber optic system connected to the Horiba-Jovin Ybon Fluoromax 4 spectrofluorimetric exciting at appropriated λ (nm) the solid compounds. All the measurements were performed at 298 K. Luminescence quantum yields were measured using a solution of quinine sulphate in sulphuric acid (0.5 M) as a standard [ϕ] = 0.54 and were corrected for different refraction indexes of solvents [28].

3.3. Computational methods

Density Functional Theory (DFT) in the Kohn–Sham approximation was used to optimize the geometry of all the species modeled. The hybrid exchange–correlation functional with a long range correction, CAM-B3LYP [29] was used through all the calculations with the def2-svp basis set [30] for every atom and the ecp-60-mwb electron core potential for mercury [31]. The stability of the wave function and the hessian were calculated on the optimized geometries at the same level to establish that both the optimized geometry and the optimized wave function correspond to a minimum. Non-specific solvent effects were partially taken into account using a continuum model, PCM, with ethanol as the chosen dielectric. All the calculations have been performed using the Gaussian09 suite of programs [32].

3.4. Chemicals and starting materials

$Cu(CF_3SO_3)_2$, $Ni(BF_4)_2$, $Hg(CF_3SO_3)_2$, $Zn(CF_3SO_3)_2$, $Ca(ClO_4)_2$ and $NaNO_3$ were purchased from Alfa Aesar and Sigma–Aldrich. All were used without further purification. All solvents were purchased from PANREAC and Riedel-de Häen and used without further purification.

The synthesis of organic ligands **L1** to **L3** was published recently [17,18].

3.5. Synthesis of ligand L4

The starting compound *bis*-[*N*-*t*-butyloxycarbonyl [2-(thien-2′-yl)benzoxazol-5-yl]-L-alanine methyl ester] [19] (0.080 g, 1.54×10^{-4} mol) was dissolved in 1,4-dioxane (1 mL), in an ice bath, and sodium hydroxide 1 M aqueous solution (0.23 mL, 2.3×10^{-4} mol, 1.5 eq) was added drop wise. The mixture was stirred at room temperature for 3 h. The pH was adjusted to 2–3 by addition of $KHSO_4$ 1 M aqueous solution and extracted with ethyl acetate (3×10 mL). After drying with anhydrous magnesium sulphate and evaporation of the solvent, the residue was triturated with diethyl ether and a yellow solid was obtained.

Colour: Yellow powder, melting point = 98 °C, *Anal.* Calc. for $C_{34}H_{36}N_4O_{10}S_2$ (MW = 692.2): C, 58.95; H, 5.25; N, 8.10; S, 4.65. Found: C, 59.15; H, 5.45; N, 8.15; S, 4.70% CHNS. IR (NaCl windows): ν (NH st) (cm^{-1}) = 3310; ν (COO^- st) (cm^{-1}) = 1745, ν (C=O) (cm^{-1}) = 1698; ν (C=C benzene) (cm^{-1}) = 1660; ν (–CH_2 δ) (cm^{-1}) = 1452; ν (–CH_3 δ) (cm^{-1}) = 1372; ν (C–O–C cyclic ethers) (cm^{-1}) = 1260,1229; ν (thiophene) (cm^{-1}) = 3065 (CH st), 1538 (CH γ), 751 (CH δoop).

MS (MALDI-TOF-MS) *m/z* without matrix: 693.56 $[L4H]^+$.

3.6. Synthesis of metal complexes – general procedure

Two equivalents of the appropriate metal salt of copper(II), nickel(II) or mercury(II) (0.26 mmol, 0.34 mmol, 0.26 mmol) were dissolved in abs. ethanol (5 mL) and added dropwise to a stirred solution of the ligand (0.13 mmol L_1, 0.17 mmol L_2, 0.13 mmol L_3) in absolute ethanol. The solution was gently heated and stirred over-night. The solvent was evaporated under vacuum until *ca.* 2 mL. Diethyl ether was added to the solution and the resulting solid products were isolated by filtration, washed with cold absolute ethanol, diethyl ether, and dried under vacuum. All complexes appear to be air stable soluble in DMSO, DMF, CH_3CN, $CHCl_3$, absolute CH_3OH but insoluble in water.

3.6.1. $[Cu_2L1](CF_3SO_3)_4{\cdot}2CH_3CN{\cdot}2H_2O$ (**1**)

Colour: green. Yield: 27%. *Anal.* Calc. for $C_{27}H_{30}Cu_2F_{12}N_4O_{19}S_5$ (MW: 1227.85): C, 26.35; H, 2.45; Cu, 10.33; N, 4.55; S, 13.04. Found: C, 26.33; H, 2.50; Cu, 10.70; N, 4.55; S, 12.95%. IR (KBr, cm^{-1}): 1619 [ν(C=O)], 1574 [ν(C=C)], 1480, 1418 [ν(C=N)], 1253 [$\nu(C–O)_{benzoxazol}$]. MS (MALDI-TOF-MS) *m/z*: 451.03 $[L1Cu]^+$; 510.08 $[L1Cu.CH_3CN.H_2O]^+$; 1150.80 $[L1(Cu_2(CF_3SO_3)_4).CH_3CN]^+$. UV–Vis in abs. ethanol (λ nm): 315 nm, ($\varepsilon \approx 4.58$). Fluorescence emission band in abs. ethanol (λ_{exc} = 315 nm); λ_{emis} = 384 nm.

3.6.2. $[Ni_2L1]\ (BF_4)_4{\cdot}7H_2O$ (**2**)

Colour: brown. Yield: 51%. *Anal.* Calc. for $C_{19}H_{34}B_4F_{16}Ni_2N_2O_{12}S$ (MW: 978.07): C, 23.30; H, 3.50; N, 2.85; Ni, 11.99; S, 3.25. Found: C, 23.35; H, 3.60; N, 3.10; Ni, 12.25; S, 3.25%. IR (KBr, cm^{-1}): 1619 [ν(C=O)], 1577 [ν(C=C)], 1415 [ν(C=N)], 1259 [$\nu(C–O)_{benzoxazol}$]. MS (MALDI-TOF-MS) *m/z*: 446.05 $[L1Ni]^+$; 678.05 $[L1Ni_2(BF_4)_2]^+$ UV–Vis in abs. ethanol (λ nm): 316 nm, ($\varepsilon \approx 4.40$). Fluorescence emission band in abs. ethanol (λ_{exc} = 315 nm); λ_{emis} = 384 nm.

3.6.3. $[Hg_2L1]\ (CF_3SO_3)_4{\cdot}4H_20$ (**3**)

Colour: brown. Yield: 35%. *Anal.* Calc. for $C_{23}H_{28}F_{12}\ Hg_2N_2O_{21}S_5$ (MW: 1459.90): C, 18.95; H, 1.95; Hg, 27.50; N, 1.90; S, 11.00. Found: C, 18.65; H, 1.75; Hg, 27.75; N, 2.10; S, 11.20%. IR (KBr, cm^{-1}): 1625 [ν(C=O)], 1579 [ν(C=C)], 1439 [ν(C=N)], 1256 [$\nu(C–O)_{benzoxazol}$]. MS (MALDI-TOF-MS) *m/z*: 590.07 $[L1Hg]^+$; 843.65 $[L1Hg_2{\cdot}3H_2O]^+$. UV–Vis in abs. ethanol (λ nm): 320 nm, ($\varepsilon \approx 4.39$). Fluorescence emission band in abs. ethanol (λ_{exc} = 320 nm); λ_{emis} = 386 nm.

3.6.4. $[Cu_2L2](CF_3SO_3)_4{\cdot}3H_2O$ (**4**)

Colour: green. Yield: 37%. *Anal.* Calc. for $C_{18}H_{18}Cu_2F_{12}N_2O_{18}S_5$ (MW: 1063.76): C, 20.30; H, 1.70; Cu, 11.93; N, 2.63; S, 15.04. Found: C, 20.25; H, 1.15; Cu, 12.03; N, 2.85; S, 15.00%. IR (KBr, cm^{-1}): 1605 [ν(C=O)], 1573 [ν(C=C)], 1439 [ν(C=N)], 1256 [$\nu(C–O)_{benzoxazol}$]. MS (MALDI-TOF-MS) *m/z*: 518.95 $[L2Cu(CF_3SO_3).H_2O]^+$; 862.65 $[L2Cu_2(CF_3SO_3)_3]^+$. UV–Vis bands in abs. ethanol (λ nm): 315 nm, ($\varepsilon \approx 4.30$). Fluorescence emission band in abs. ethanol (λ_{exc} = 315 nm); λ_{emis} = 384 nm.

3.6.5. $[Ni_2L2](BF_4)_4{\cdot}6H_2O$. (**5**)

Colour: green. Yield: 61%. *Anal.* Calc. for $C_{14}H_{23}B_4F_{16}Ni_2N_2O_9S$ (MW: 860.01): C, 19.55; H, 2.80; N, 3.25; Ni, 13.65; S, 3.70. Found: C, 20.15; H, 2.45; N, 3.60; Ni, 13.45; S, 3.45%. IR (KBr, cm^{-1}): 1605 [ν(C=O)], 1579 [ν(C=C)], 1439 [ν(C=N)], 1256 [$\nu(C–O)_{benzoxazol}$]. MS (MALDI-TOF-MS) *m/z*: 347.00 $[L2Ni]^+$; 490.95 $[L2Ni_2(BF_4)]^+$. UV–Vis band in abs. ethanol (λ nm): 315 nm, ($\varepsilon \approx 4.24$). Fluorescence emission band in abs. ethanol (λ_{exc} = 315 nm); λ_{emis} = 384 nm.

3.6.6. $[Hg_2L2](CF_3SO_3)_4{\cdot}2CH_3CN{\cdot}2H_2O$ (**6**)

Colour: yellow. Yield: 25%. *Anal.* Calc. for $C_{22}H_{22}F_{12}Hg_2N_4O_{17}S_5$ (MW: 1405.88): C, 18.85; H, 1.60; Hg, 28.58; N, 3.99; S, 11.45.

Found: C, 19.05; H, 1.45; Hg, 28.65; N, 4.15; S, 11.35%. IR (KBr, cm^{-1}): 1614 [ν(C=O)], 1576 [ν(C=C)], 1438 [ν(C=N)], 1256 [ν(C–O)$_{benzoxazol}$]. MS (MALDI-TOF-MS) *m/z*: 638.90 $[L2Hg(CF_3SO_3)]^+$; 828.95 $[L2Hg(CF_3SO_3)_2{\cdot}CH_3CN]^+$; 1136.75 $[L2Hg_2(CF_3SO_3)_3]^+$. UV–Vis bands in abs. ethanol (λ nm): 315 nm, log $\varepsilon \approx 4.24$. Fluorescence emission band in abs. ethanol (λ_{exc} = 315 nm); λ_{emis} = 384 nm.

3.6.7. $[Ni_2L3]\,(BF_4)_4{\cdot}4H_2O$ **(7)**

Colour: yellow-green. Yield: 23%. *Anal.* Calc. for $C_{18}H_{22}B_4F_{16}N_2Ni_2O_7S_2$ (MW: 905.96): C, 23.83; H, 2.45; N, 3.10; Ni, 12.95; S, 7.10. Found: C, 23.60; H, 2.90; N, 3.15; Ni, 13.25; S, 7.55%. IR (KBr, cm^{-1}): 1605 [ν(C=O)], 1573 [ν(C=C)], 1439 [ν(C=N)], 1256 [ν(C–O)$_{benzoxazol}$]. MS (MALDI-TOF-MS) *m/z*: 602.74 $[L3Ni(BF_4)_2]^+$; 697.45 $[L3Ni_2(BF_4)_2{\cdot}2H_2O]^+$. UV–Vis bands in abs. ethanol (λ nm): 316 nm, log $\varepsilon \approx 4.35$. Fluorescence emission band in abs. ethanol (λ_{exc} = 316 nm); λ_{emis} = 386 nm.

3.6.8. $[Cu_2L3]\,(CF_3SO_3)_4{\cdot}3H_2O$ **(8)**

Colour: green. Yield: 22%. *Anal.* Calc. for $C_{22}H_{20}Cu_2F_{12}N_2O_{18}S_6$ (MW: 1145.74): C, 23.05; H, 1.75; N, 2.45; Cu, 11.07; S, 16.76. Found: C, 23.20; H, 1.90; N, 2.35; Cu, 11.25; S, 17.05%. IR (KBr, cm^{-1}): 1602 [ν(C=O)], 1575 [ν(C=C)], 1439 [ν(C=N)], 1255 [ν(C–O)$_{benzoxazol}$]. MS (MALDI-TOF-MS) *m/z*: 732.38 $[L3Cu(CF_3SO_3)_2]^+$; 831.70 $[L3Cu_2(CF_3SO_3)_2{\cdot}2H_2O]^+$. UV–Vis bands in abs. ethanol (λ nm): 315 nm, log $\varepsilon \approx 4.45$. Fluorescence emission band in abs. ethanol (λ_{exc} = 315 nm); λ_{emis} = 386 nm.

Acknowledgments

We are indebted to InOU Uvigo by project K914 122P 64702 (Spain) and FCT – Portugal by project PTDC/QUI/66250/2006 for financial support. C.L. thanks Xunta de Galicia, Spain, for the Isidro Parga Pondal Research Program. E.O. thanks to FC-MCTES (Portugal) by her Ph.D. grant SFRH/BD/35905/2007, and to Fundação Calouste Gulbenkian (Portugal), for the National Prize in creativity and quality in research activity, 2008. We also thank the CESGA (Centro de Supercomputación de Galicia) for generous allocation of computational resources. We are grateful to Dr. José Luis Capelo from the University of Vigo, Spain for the help with the MALDI-TOF-MS spectra.

References

[1] A. Pasini, L.J. Casella, Inorg. Nucl. Chem. 36 (1979) 2133.
[2] V.J. Derose, S. Burns, N.K. Kim, M. Vogt, Compr. Coord. Chem. II 8 (2004) 787.
[3] S.J. Lippard, J.M. Berg, Principles of Bioinorganic Chemistry, University Science Books, Sausalito, CA, 1994.
[4] H. Umezawa, Prog. Biochem. Pharmacol. 11 (1976) 18.
[5] P.R. Chetana, R, Rao, M. Roy, A.K. Patra, Inorg. Chim. Acta 362 (2009) 4692.
[6] M.N. Hosny, Transition. Met. Chem. 32 (2007) 117.
[7] N. Grosser, S. Oberle, G. Berndt, K. Erdmannk, A. Hemmerle, Biochem. Biophys. Res. Commun. 314 (2004) 351.
[8] J. Chin, Acc. Chem. Res. 24 (1991) 145.
[9] J. Suh, Acc. Chem. Res. 25 (1992) 273.
[10] J. Gallagher, O. Zelenko, A.D. Walts, D.S. Sigman, Biochemistry 37 (1998) 2096.
[11] E.L. Hegg, J.N. Burstyn, J. Am. Chem. Soc. 117 (1995) 7015.
[12] T.M. Rana, Adv. Inorg. Biochem. 10 (1993) 177.
[13] V. Anbalagan, V.M.J. Stipdonk, J. Mass Spectrom. 38 (2003) 982.
[14] M.M. Yamashita, L. Wesson, G. Eisenman, D. Eisenberg, Proc. Natl. Acad. Sci. USA 87 (1990) 5648.
[15] T. Marine, N. Russo, M. Toscano, J. Mass Spectrom. 37 (2002) 786.
[16] (a) C. Lodeiro, J.L. Capelo, J.C. Mejuto, E. Oliveira, H.M. Santos, B. Pedras, C. Nuñez, Chem. Soc. Rev. 39 (2010) 2948;
(b) C. Lodeiro, F. Pina, Coord. Chem. Rev. 253 (2009) 1353;
(c) L. Rodriguez, C. Lodeiro, J.C. Lima, R. Crehuet, Inorg. Chem. 47 (2008) 4952;
(d) R.M.F. Batista, E. Oliveira, S.P.G. Costa, C. Lodeiro, M.M.M. Raposo, Org. Lett. 9 (2007) 3201.
[17] S.P.G. Costa, E. Oliveira, C. Lodeiro, M.M.M. Raposo, Sensors 7 (2007) 2096.
[18] S.P.G. Costa, E. Oliveira, C. Lodeiro, M.M.M. Raposo, Tetrahedron Lett. 49 (2008) 5258.
[19] S.P.G. Costa, R.M.F. Batista, M.M.M. Raposo, Tetrahedron 64 (2008) 9733.
[20] (a) J.L. Capelo, A.V. Filgueiras, I. Lavilla, C. Bendicho, Talanta 50 (1999) 905;
(b) C. Fernandez, A.C.L. Conceição, R. Rial-Otero, C. Vaz, J.L. Capelo, Anal. Chem. 78 (2006) 2494;
(c) A. Tamayo, B. Pedras, C. Lodeiro, L. Escriche, J. Casabó, J.L. Capelo, B. Covelo, R. Sillanpää, R. Kivekäs, Inorg. Chem. 46 (2007) 7818.
[21] R.M. Silverstein, G.C. Bassler, T.C. Morrill, Spectrometric Identification of Organic Compounds, fourth ed., John Wiley & Sons, New York, 1981.
[22] C. Núñez, R. Bastida, A. Macías, E. Bértolo, L. Fernandes, J.L. Capelo, C. Lodeiro, Tetrahedron 65 (2009) 6179.
[23] K. Ruckak, Spectrochim. Acta A 57 (2001) 2161.
[24] A.W. Czarnik, Fluorescent Chemosensors for Ion and Molecule Recognition, American Chemical Society, Washington, DC, 1993.
[25] A.P. de Silva, H.Q.N. Gunaratne, T. Gunnlaugsson, A.J.M. Huxley, C.P. McCoy, J.T. Rademacher, T.E. Rice, Chem. Rev. 97 (1997) 1515.
[26] (a) J.S. Casas, M.S. García-Tasende, J. Sordo, Coord. Chem. Rev. 209 (2000) 197;
(b) .G. Kuzmina, Yu.T. Struchkov, E.M. Rokhlina, D.N. Kravtsov, J. Struct. Chem. 24 (1983) 130;
(c) Z. Popovic, D. Matkovic-Calogovic, Z. Soldin, G. Pavlovic, N. Davidovic, D. Vikic-Topic, Inorg. Chim. Acta 294 (1999) 35;
(d) S.S. Lemos, D.U. Martins, V.M. Deflon, J. Elena, J. Organomet. Chem. 694 (2009) 253;
(e) M. Kato, K. Kojima, T. Okamura, H. Yamamoto, T. Yamamura, N. Ueyama, Inorg. Chem. 44 (2005) 4037;
(f) P. Fernandez, A. Sousa-Pedrares, J. Romero, J.A. Garcia-Vazquez, A. Sousa, P. Perez-Lourido, Inorg. Chem. 47 (2008) 2121.
[27] P. Gans, A. Sabatini, A. Vacca, Talanta 43 (1996) 1739.
[28] I.B. Berlman, Handbook of Fluorescence Spectra of Aromatic Molecules, second ed., Academic Press, New York, 1971.
[29] T. Yanai, D.P. Tew, N.C. Handy, Chem. Phys. Lett. 393 (2004) 51.
[30] F. Weigend, R. Ahlrichs, J. Phys. Chem. Chem. Phys. 7 (2005) 3297.
[31] D. Andrae, U. Haussermann, M. Dolg, H. Stoll, H. Preuss, Theor. Chim. Acta 77 (1990) 123.
[32] M.J. Frisch, G.W. Trucks, H.B. Schlegel, G.E. Scuseria, M.A. Robb, J.R. Cheeseman, G. Scalmani, V. Barone, B. Mennucci, G.A. Petersson, H. Nakatsuji, M. Caricato, X. Li, H.P. Hratchian, A.F. Izmaylov, J. Bloino, G. Zheng, J.L. Sonnenberg, M. Hada, M. Ehara, K. Toyota, R. Fukuda, J. Hasegawa, M. Ishida, T. Nakajima, Y. Honda, O. Kitao, H. Nakai, T. Vreven, J.A. Montgomery Jr., J.E. Peralta, F. Ogliaro, M. Bearpark, J.J. Heyd, E. Brothers, K.N. Kudin, V.N. Staroverov, R. Kobayashi, J. Normand, K. Raghavachari, A. Rendell, J.C. Burant, S.S. Iyengar, J. Tomasi, M. Cossi, N. Rega, J.M. Millam, M. Klene, J.E. Knox, J.B. Cross, V. Bakken, C. Adamo, J. Jaramillo, R. Gomperts, R.E. Stratmann, O. Yazyev, A.J. Austin, R. Cammi, C. Pomelli, J.W. Ochterski, R.L. Martin, K. Morokuma, V.G. Zakrzewski, G.A. Voth, P. Salvador, J.J. Dannenberg, S. Dapprich, A.D. Daniels, Ö. Farkas, J.B. Foresman, J.V. Ortiz, J. Cioslowski, D.J. Fox, Gaussian 09, Revision A.1, Gaussian, Inc., Wallingford, CT, 2009.